

Efficient Many-Body Non-Markovian Dynamics of Organic Polaritons

Piper Fowler-Wright^{1D}, Brendon W. Lovett^{1D}, and Jonathan Keeling^{1D}

SUPA, School of Physics and Astronomy, University of St. Andrews, St. Andrews, KY16 9SS, United Kingdom

(Received 20 December 2021; revised 23 May 2022; accepted 24 August 2022; published 21 October 2022)

We show how to simulate a model of many molecules with both strong coupling to many vibrational modes and collective coupling to a single photon mode. We do this by combining process tensor matrix product operator methods with a mean-field approximation which reduces the dimension of the problem. We analyze the steady state of the model under incoherent pumping to determine the dependence of the polariton lasing threshold on cavity detuning, light-matter coupling strength, and environmental temperature. Moreover, by measuring two-time correlations, we study quadratic fluctuations about the mean field to calculate the photoluminescence spectrum. Our method enables one to simulate many-body systems with strong coupling to multiple environments, and to extract both static and dynamical properties.

DOI: 10.1103/PhysRevLett.129.173001

The strong coupling between organic matter confined in a microcavity and light results in new collective modes—superpositions of molecular excitations and photons known as exciton polaritons [1]. Under sufficient pumping, these may condense into a coherent or lasing state, as has now been demonstrated in a diverse range of organic materials [2–7] (see Ref. [1] for a review). The rich photophysics of organic molecules allows for the possibility of room temperature lasing devices with ultralow thresholds, yet also makes the task of determining the optimal conditions for lasing a challenging one. In particular, one must consider the effect on the dynamics of the vibrational environment of each molecule [8], which is generally structured and beyond weak coupling or Markovian treatments [9–17]. To this end there have been studies of polariton condensation using simplified models with a few vibrational modes [8,18–27], and also studies involving exact vibrational spectra for a small number of molecules [15,16]. However, the real system has both a complex vibrational density of states and many, e.g., 10^5 , molecules. Therefore, what is needed is a method capable of handling large systems with non-Markovian effects. Here we provide such a method and show the consequences for the description of polariton lasing.

Process tensor matrix product operator (PT-MPO) methods are a class of numerical methods based upon the process tensor (PT) description of open quantum system dynamics [28–34]. The PT captures all possible effects of the environment on a system. The system Hamiltonian propagator, or any system operator, then forms a finite set of interventions that may be contracted with the PT and thus one can find any system observable or multitime correlation function. Crucially, the PT can be represented efficiently as a matrix product operator that only needs to be calculated once for a given system-bath interaction and set of bath conditions [31]. While this provides an efficient means to

evolve a system with long memory times, such methods have so far been limited to systems of small Hilbert space dimension.

In this Letter we present a mean-field approach to reduce an N -body problem to one that can be handled by PT-MPO methods without further approximation. This approach does not require expressions for the system eigenstates and energies, and allows for genuine non-Markovian dynamics of many-body systems. As we will discuss, mean-field theory consists of the ansatz that there are no correlations between certain parts of the system. Here we employ this approach to accurately treat the vibrational environments of a many-molecule–cavity system. In particular, we develop a realistic model of an organic laser based on BODIPY-Br [Figs. 1(a) and 1(b)], an organic molecule which has shown polariton lasing [5,7]. We find results that differ significantly from those obtained in the model where the vibrational environments cause simple dephasing—a model that cannot account for lasing in the presence of strong light-matter coupling. We determine how modifying the light-matter coupling and environmental temperature of our model changes the lasing threshold, and calculate the observed photoluminescence.

We model N identical molecules as a collection of two-level systems (Pauli matrices σ_i^α) interacting with a single near-resonant cavity mode (bosonic operator a) according to the Dicke Hamiltonian under the rotating-wave approximation. Setting $\hbar = 1$, the system Hamiltonian is

$$H_S = \omega_c a^\dagger a + \sum_{i=1}^N \left[\frac{\omega_0}{2} \sigma_i^z + \frac{\Omega}{2\sqrt{N}} (a\sigma_i^+ + a^\dagger \sigma_i^-) \right] \quad (1)$$

where ω_0 and ω_c are the two-level system and cavity frequencies, and σ_i^+ (σ_i^-) the raising (lowering) operator for the i th spin. The collective coupling Ω controls the

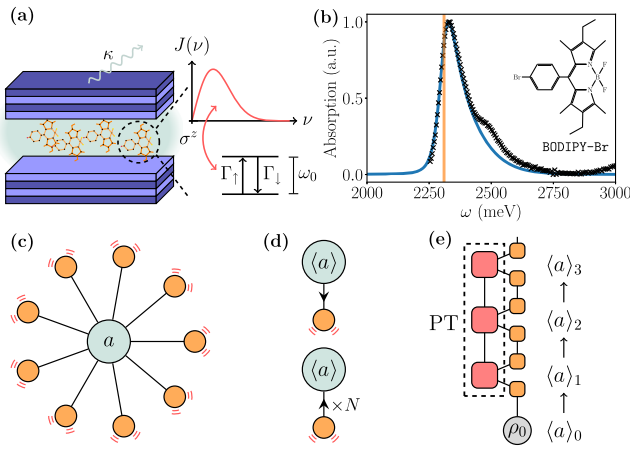


FIG. 1. (a) Our system: a molecular ensemble in an optical microcavity. Each molecule is modeled as a driven-dissipative two-level system with a diagonal coupling to a harmonic environment. The spectral density $J(\nu)$ of the environment is chosen to match (b) absorption data [5] for BODIPY-Br at 300 K (black crosses: experimental data, blue curve: model spectrum, orange line: $\omega_0 = 2310$ meV). For the Ohmic form Eq. (3) with dissipation $\Gamma_\downarrow = 10$ meV we obtained $\alpha = 0.25$ and $\nu_c = 150$ meV ($\hbar = 1$). (c) Schematic of the many-body open system before and (d) after the mean-field reduction. (e) Tensor network for the PT-MPO method with the concurrent dynamics of the cavity field. The PT (red) is constructed independently of the system propagators (orange) and initial state (gray), allowing the dynamics for many different system Hamiltonians to be calculated at relatively little cost.

light-matter interaction such that the bright eigenstates of H_S , i.e., the polaritons, are split as $\pm\Omega/2$ at resonance.

The Hamiltonian Eq. (1) may be referred to as the Tavis-Cummings model. Its extension to include a single vibrational mode, the Holstein-Tavis-Cummings model, has frequently been used to describe cavity bound organic emitters [18,19,21–23,25–27]. We instead consider the interaction of each two-level system with a *continuum* of modes represented by the harmonic environment

$$H_E^{(i)} = \sum_j \left[\nu_j b_j^\dagger b_j + \frac{\xi_j}{2} (b_j + b_j^\dagger) \sigma_i^z \right], \quad (2)$$

where b_j is the annihilation operator for the j th mode of frequency ν_j . The system-environment coupling is characterized by a spectral density $J(\nu) = \sum_j (\xi_j/2)^2 \delta(\nu - \nu_j)$, taken to be Ohmic in the form

$$J(\nu) = 2\alpha\nu e^{-(\nu/\nu_c)^2}, \quad \nu > 0, \quad (3)$$

where α and ν_c are chosen to reproduce the leading structure of the absorption spectrum of BODIPY-Br at $T = 300$ K [Fig. 1(b)]. This effectively captures the low frequency modes arising from the host matrix of the molecule. The realistic picture of vibrational dephasing

it affords is the most significant advancement of our Letter. In the limit that the system-environment coupling is weak one might look to derive a Redfield theory [35]. However, as we discuss in the Supplemental Material [36], this is difficult in the presence of strong light-matter coupling.

Finally we consider incoherent pump Γ_\uparrow and dissipation Γ_\downarrow of the two-level systems as well as field decay κ . Since these are associated with baths at optical frequencies (e.g., 10^{15} Hz) they may be well approximated [35] by Markovian terms in the master equation for the total density operator ρ ,

$$\begin{aligned} \partial_t \rho = -i & \left[H_S + \sum_{i=1}^N H_E^{(i)}, \rho \right] + 2\kappa \mathcal{L}[a] \\ & + \sum_{i=1}^N (\Gamma_\uparrow \mathcal{L}[\sigma_i^+]) + \Gamma_\downarrow \mathcal{L}[\sigma_i^-]), \end{aligned} \quad (4)$$

with $\mathcal{L}[x] = x\rho x^\dagger - \{x^\dagger x, \rho\}/2$. If $H_E^{(i)}$ is absent one recovers the Tavis-Cummings model with pumping and decay which, as we discuss below, requires inversion $\Gamma_\uparrow > \Gamma_\downarrow$ to show lasing. Below we fix Γ_\downarrow and κ and observe the transition of the system from a normal state, where the expectation $\langle a \rangle$ of the photon operator vanishes, to a lasing state, where $\langle a \rangle$ is nonzero and time dependent, as Γ_\uparrow is increased from zero.

Simulating dynamics in the presence of strong coupling to a structured environment is a computationally intense task and as such PT-MPO methods cannot be used to solve for a large number of open systems simultaneously. Our strategy is to use mean-field theory to reduce the N -molecule-cavity system to a single molecule interacting with a coherent field [Figs. 1(c) and 1(d)].

According to mean-field theory, we assume a product state for the many-body density operator ρ , i.e., a factorization between the photon and individual molecules, an ansatz known [61,62] to be exact as $N \rightarrow \infty$. This reduces the problem to the coupled dynamics of the molecular mean-field Hamiltonian

$$H_{MF} = \frac{\omega_0}{2} \sigma^z + \frac{\Omega}{2\sqrt{N}} (\langle a \rangle \sigma^+ + \langle a \rangle^* \sigma^-), \quad (5)$$

combined with evolution of the field expectation

$$\partial_t \langle a \rangle = -(i\omega_c + \kappa) \langle a \rangle - i \frac{\Omega\sqrt{N}}{2} \langle \sigma^- \rangle. \quad (6)$$

Here $\langle \sigma^- \rangle$ (no subscript) is the average of any one of the identical spins. Thus, by propagating a *single* spin with H_{MF} and subject to the vibrational environment and individual losses described above, we can effectively simulate the N -molecule system using a PT-MPO method provided that at each time step we also evolve $\langle a \rangle$

according to Eq. (6) [Fig. 1(d)]. In Ref. [36] we discuss the derivation of Eqs. (5) and (6) further as well as the role of “bright” and “dark” excitonic states [8,23,24,63–65] in mean-field theory.

To calculate the dynamics we use the PT-MPO provided by the time evolving MPO (TEMPO) method [28,31,66,67]. Notable to our problem is that the system propagators depend on the field $\langle a \rangle$, which depends self-consistently on the state of the system. A second-order Runge-Kutta method is used to integrate the field from t_n to t_{n+1} whence it may be used in the construction of the system propagator for the next time step. Further implementation details are provided in Ref. [36]. Importantly the construction of the PT capturing the influence of the bath, which is the costly part of the calculation, only needs to be performed once for a given spectral density Eq. (3) and bath temperature T . It can then be reused with many different system Hamiltonians or parameters. This is particularly advantageous when one wishes to vary one or more system parameters to map out a phase diagram.

Figure 2(a) shows time evolution simulations at $\Omega = 200$ meV and a small negative detuning $\Delta = \omega_c - \omega_0 = -20$ meV. For each run the bath was prepared in a thermal state at $T = 300$ K and the spin pointing down, with a

small initial field to avoid the trivial fixed point of Eqs. (5) and (6). The dynamics were generated up to a time $t_f = 1.3$ ps and the final value $\langle a \rangle_f$ recorded. This gave the steady-state field except near the phase boundary where, due to the critical slowing down associated with a second-order transition, $\langle a \rangle$ was still changing at t_f . To accommodate this, an exponential fit was made to the late time dynamics yielding an estimate of the steady-state value indicated by filled circles in Fig. 2(b). Where this was not possible (i.e., the fitting failed), the final value of the field is marked with a cross and the attempted fit with an open circle. An automated procedure [36] was used to assess fit validity and any point with an invalid fit was not used in subsequent calculations.

Having obtained the steady-state field for a number of pump strengths encompassing the transition [Fig. 2(b)], a second fitting was performed to extract the threshold pump Γ_c at each detuning. This was repeated for different light-matter coupling strengths and temperatures to produce the phase diagrams Figs. 2(c) and 2(d).

In Fig. 2(c), we study the evolution of the threshold Γ_c as the coupling Ω increases. At the smallest coupling considered, $\Omega = 100$ meV, the threshold is high and for $\Gamma_\uparrow \leq \Gamma_\downarrow$ there is only a small window of detunings for which lasing is supported—i.e., the photon frequency coincides with a region of net gain in the spectrum [69]. This curve may be compared with the prediction of weak light-matter coupling theory [36] shown with a gray dashed line. The disagreement here, most apparent nearer zero detuning, reflects the fact that $\Omega = 100$ meV is already beyond weak light-matter coupling.

We note the observed behavior cannot be described by a weak system-bath coupling model in which the coupling to the bath is replaced by Markovian (temperature dependent) dephasing. Indeed, such a model requires $\Gamma_\uparrow > \Gamma_\downarrow$ for lasing and predicts a phase diagram that is symmetric about $\Delta = 0$ [36]. The same is true for models that completely neglect the effect of vibrational modes [70]. The existence of lasing for $\Gamma_\uparrow < \Gamma_\downarrow$ within our model is a consequence of the vibrational bath. The detuning for minimum threshold evolves with Ω and is not simply set by the peak of the molecular emission spectrum; this is due to reabsorption of cavity light playing a role for the parameters we consider [71].

As the light-matter coupling increases, faster emission into the cavity mode sees the threshold reduce before eventually saturating. The threshold becomes less dependent on detuning as lasing is now dictated by whether the frequency of the lower polariton formed coincides with a region of gain in the spectrum, and this occurs for a larger range of cavity frequencies. Similar observations were made in models with sharp vibrational resonances [26]. In that work reentrance under Γ_\uparrow was seen—behavior absent here because of the broader molecular spectrum we consider.

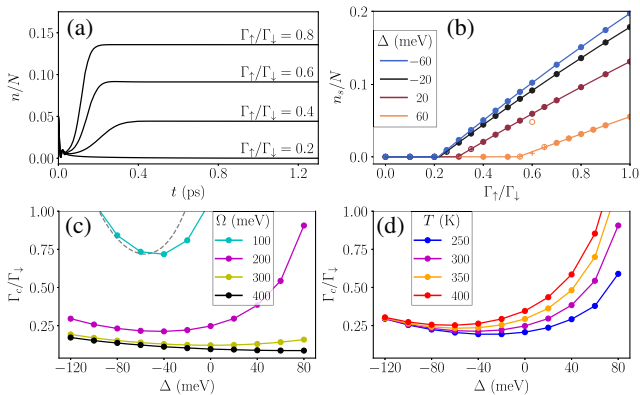


FIG. 2. Determining the threshold of an organic laser. (a) Example dynamics of the scaled photon number $n/N = |\langle a \rangle|^2/N$ below ($\Gamma_\uparrow = 0.2\Gamma_\downarrow$) and above ($\Gamma_\uparrow \geq 0.4\Gamma_\downarrow$) the lasing transition at $\Omega = 200$ meV, $T = 300$ K, and $\Delta = \omega_c - \omega_0 = -20$ meV (note n scales with N above threshold [68]). The losses were fixed at $\kappa = \Gamma_\downarrow = 10$ meV. Initial conditions: the system was prepared in a σ^z -down state with $n_0/N = 0.05$ and the bath in a thermal state. Computational parameters and convergence information are provided in Ref. [36]. (b) Steady-state photon number with pump strength at $\Omega = 200$ meV, $T = 300$ K for several different detunings (closed circle: steady-state value obtained from a valid fit of late time behavior, open circle: invalid fit, cross: final value). Fitting a curve to the data at each detuning provided an estimate of the threshold Γ_c . This was repeated for different Ω and T to produce (c) and (d), respectively. The result of a weak-coupling calculation [36] for $\Omega = 100$ meV is included in (c) as a dashed gray line.

A key question in the study of organic polaritons is to what extent thermalization occurs, and thus how temperature affects the threshold [1,71]. Motivated by this and the range of temperatures accessible in organic polariton experiments we examine the dependence of threshold on environmental temperature T at fixed $\Omega = 200$ meV. Changing T shifts, and increases the width of, the molecular spectrum. The result for the phase diagram, shown in Fig. 2(d), is a suppression of lasing with increasing T , most significantly for positive detunings where the lower polariton is more excitonic. This temperature dependence is one aspect of the phase diagram that cannot generally be captured by simplified models with a few vibrational modes, as we demonstrate in Ref. [36].

We next study quadratic fluctuations about the mean field, as described by two-time correlations and their Fourier transforms. Specifically we calculate the spectral weight and the photoluminescence (PL) spectrum, the latter of which is the actual measured observable in all polariton experiments [1]. Multitime correlations are naturally accessible within the PT-MPO framework, allowing us to calculate absorption and emission spectra without recourse to the quantum regression theorem.

We use that the retarded D^R and Keldysh D^K photon Green's functions may be written in terms of the exciton self-energies [65,72]

$$\Sigma^{-+}(\omega) = \frac{i\Omega^2}{4} \int_0^\infty dt e^{i\omega t} \langle [\sigma^-(t), \sigma^+(0)] \rangle, \quad (7)$$

$$\Sigma^{--}(\omega) = \frac{i\Omega^2}{4} \int_{-\infty}^\infty dt e^{i\omega t} \langle \{\sigma^-(t), \sigma^+(0)\} \rangle. \quad (8)$$

The photon Green's functions then take the form

$$D^R(\omega) = \frac{1}{\omega - \omega_c + i\kappa + \Sigma^{-+}(\omega)}, \quad (9)$$

$$D^K(\omega) = -\frac{\Sigma^{--}(\omega) + 2i\kappa}{|\omega - \omega_c + i\kappa + \Sigma^{-+}(\omega)|^2}. \quad (10)$$

Hence, by calculating the correlators $\langle \sigma^-(t) \sigma^+(0) \rangle$ and $\langle \sigma^+(t) \sigma^-(0) \rangle$ using the PT-MPO approach, we can find the Green's functions D^R and D^K which fully characterize the spectrum of the nonequilibrium system.

Thus far we have considered a model with a single photon mode for which mean-field theory is exact as $N \rightarrow \infty$. However, it is straightforward to extend our analysis to include multiple photon modes, where the mean field can still provide a good approximation [36]. Hence we consider the model with cavity mode term $\sum_k \omega_{c,k} a_k^\dagger a_k$, where $\omega_{c,k} = \omega_c + k^2/2m_{ph}$ (recall $\hbar = 1$), and light-matter interaction $\sum_k \Omega a_k^\dagger e^{ik \cdot r_n} \sigma_i^- + \text{H.c.}$ As discussed in Ref. [36], the mean-field steady-state

equations remain similar and one now has access to the photon Green's functions $D_k^R(\omega)$, $D_k^K(\omega)$ of the multimode model.

We first consider the system without pumping ($\Gamma_\uparrow = 0$) and the spectral weight [73]

$$q_k(\omega) = -2\text{Im}D_k^R(\omega). \quad (11)$$

As the system is in the normal state, $\langle \sigma^+(t) \sigma^-(0) \rangle \equiv 0$, while an exact expression for the other correlator may be found [71] as $\langle \sigma^-(t) \sigma^+(0) \rangle = e^{-i\omega_0 t - \phi(t) - (\Gamma_\downarrow/2)t}$ where

$$\phi(t) = \int_{-\infty}^\infty d\omega \frac{J(\omega)}{\omega^2} \left[2 \coth\left(\frac{\omega}{2T}\right) \sin^2\left(\frac{\omega t}{2}\right) + i \sin(\omega t) \right]. \quad (12)$$

This provides a benchmark of our numerics: Figure 3(a) shows excellent agreement between the spectral weight derived from the analytical result Eq. (12) and that from measurement of the correlator using the PT-MPO method at $k = 0$. Figure 3(b) then illustrates the k dependence of the spectrum for $\Omega = 200$ meV.

When the system is pumped, i.e., $\Gamma_\uparrow \neq 0$, no analytical results are available and it is necessary to determine both

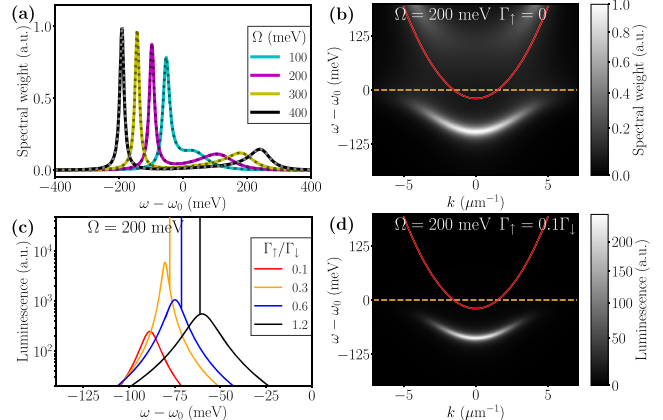


FIG. 3. (a) Spectral weight, Eq. (11), at $k = 0$ when $\Gamma_\uparrow = 0$. At each light-matter coupling, results from the analytic self-energy are shown as a dotted line, and results from PT-MPO as a solid line. (b) k -dependent spectral weight for $\Omega = 200$ meV. The bare molecular energy ω_0 is shown in orange and the photon dispersion $\omega_{c,k}$ in red (the photon mass m_{ph} was set to ω_c/c^2). (c) Photoluminescence, Eq. (13), at $k = 0$ on a logarithmic scale for four different pump strengths at $\Omega = 200$ meV. Above threshold the spin-spin correlators have a nonzero long time value giving a delta singularity, i.e., lasing peak in the spectrum, indicated here as a vertical line. Additional cross sections at smaller and larger Ω are provided in Ref. [36]. (d) k -dependent photoluminescence below threshold at $\Omega = 200$ meV and $\Gamma_\uparrow = 0.1\Gamma_\downarrow$ with red and orange lines as in (b). All panels were produced at $\Delta = -20$ meV and $T = 300$ K, with losses $\kappa = \Gamma_\downarrow = 10$ meV.

the spectrum and its occupation numerically. Here we calculate the photoluminescence [72],

$$\mathcal{L}_k(\omega) = \frac{i}{2}(D_k^K(\omega) - D_k^R(\omega) + [D_k^R(\omega)]^*). \quad (13)$$

Figure 3(c) shows $\mathcal{L}_{k=0}(\omega)$ at fixed detuning $\Delta = -20$ meV and $\Omega = 200$ meV for four different pump strengths. At the weakest pump strength, $\Gamma_{\uparrow} = 0.1\Gamma_{\downarrow}$, the system is below threshold yet $\mathcal{L}_k(\omega)$ does not vanish since, in contrast to the mean-field calculation of the steady-state photon number, the photoluminescence contains an incoherent part. Plotting the k dependence of the spectrum in this case [Fig. 3(d)] makes clear this arises from the lower polariton.

At higher pump strengths, $\Gamma_{\uparrow} = 0.3, 0.6, 1.2\Gamma_{\downarrow}$ in Fig. 3(c), the system is above threshold, with the coherent lasing contribution indicated by a delta peak superimposed on the spectrum. In particular, for $\Gamma_{\uparrow} = 0.3\Gamma_{\downarrow}$ and $0.6\Gamma_{\downarrow}$, the lasing frequency occurs noticeably to the right of the peak luminescence: the conditions to maximize \mathcal{L}_k , which depends on both the density of states and their populations, do not, in general, coincide with the point at which the lasing instability develops. We explore this further in Ref. [36] by examining the real and imaginary parts of the inverse Green's functions as the transition is approached.

In conclusion, we have developed a technique for calculating the non-Markovian dynamics of a many-body open system using mean-field theory and PT-MPO methods. We applied this technique to model the polariton lasing of an organic dye in a microcavity including many molecules with realistic vibrational spectra. This provided the steady state of the driven-dissipative system and, via the measurement of two-time correlations, its spectrum. We first determined the dependence of the threshold for lasing on cavity detuning under different light-matter coupling strengths and environmental temperatures. Second, we observed how the photoluminescence and lasing frequency of the model evolved with pump strength. For the case of a one-to-all interaction between the cavity and molecules, the mean-field treatment is exact as $N \rightarrow \infty$ [61,62]. The same applies to all-to-all networks of open systems [36,62]. More generally, there are situations where mean-field theory is not exact but offers a good approximation, including models of polariton condensation with multiple modes such as considered in Refs. [27,36,75].

The research data supporting this publication can be accessed at [79]

We thank G. E. Fux and P. Kirton from the TEMPO Collaboration for helpful discussions when implementing the mean-field approach. P. F.-W. acknowledges support from EPSRC (EP/T518062/1). B. W. L. and J. K. acknowledge support from EPSRC (EP/T014032/1).

- [1] J. Keeling and S. Kéna-Cohen, Bose-Einstein condensation of exciton-polaritons in organic microcavities, *Annu. Rev. Phys. Chem.* **71**, 435 (2020).
- [2] S. Kéna-Cohen and S. R. Forrest, Room-temperature polariton lasing in an organic single-crystal microcavity, *Nat. Photonics* **4**, 371 (2010).
- [3] J. D. Plumhof, T. Stöferle, L. Mai, U. Scherf, and R. F. Mahrt, Room-temperature Bose-Einstein condensation of cavity exciton-polaritons in a polymer, *Nat. Mater.* **13**, 247 (2014).
- [4] K. S. Daskalakis, S. A. Maier, R. Murray, and S. Kéna-Cohen, Nonlinear interactions in an organic polariton condensate, *Nat. Mater.* **13**, 271 (2014).
- [5] R. T. Grant, P. Michetti, A. J. Musser, P. Gregoire, T. Virgili, E. Vella, M. Cavazzini, K. Georgiou, F. Galeotti, C. Clark, J. Clark, C. Silva, and D. G. Lidzey, Efficient radiative pumping of polaritons in a strongly coupled microcavity by a fluorescent molecular dye, *Adv. Opt. Mater.* **4**, 1615 (2016).
- [6] C. P. Dietrich, A. Steude, L. Tropf, M. Schubert, N. M. Kronenberg, K. Ostermann, S. Höfling, and M. C. Gather, An exciton-polariton laser based on biologically produced fluorescent protein, *Sci. Adv.* **2**, e1600666 (2016).
- [7] T. Cookson, K. Georgiou, A. Zasedatelev, R. T. Grant, T. Virgili, M. Cavazzini, F. Galeotti, C. Clark, N. G. Berloff, D. G. Lidzey, and P. G. Lagoudakis, A yellow polariton condensate in a dye filled microcavity, *Adv. Opt. Mater.* **5**, 1700203 (2017).
- [8] F. Herrera and F. C. Spano, Theory of nanoscale organic cavities: The essential role of vibration-photon dressed states, *ACS Photonics* **5**, 65 (2018).
- [9] M. Thorwart, J. Eckel, J. Reina, P. Nalbach, and S. Weiss, Enhanced quantum entanglement in the non-Markovian dynamics of biomolecular excitons, *Chem. Phys. Lett.* **478**, 234 (2009).
- [10] A. Ishizaki and G. R. Fleming, Theoretical examination of quantum coherence in a photosynthetic system at physiological temperature, *Proc. Natl. Acad. Sci. U.S.A.* **106**, 17255 (2009).
- [11] J. Prior, A. W. Chin, S. F. Huelga, and M. B. Plenio, Efficient Simulation of Strong System-Environment Interactions, *Phys. Rev. Lett.* **105**, 050404 (2010).
- [12] F. Fassoli, A. Olaya-Castro, and G. D. Scholes, Coherent energy transfer under incoherent light conditions, *J. Phys. Chem. Lett.* **3**, 3136 (2012).
- [13] A. W. Chin, J. Prior, R. Rosenbach, F. Caycedo-Soler, S. F. Huelga, and M. B. Plenio, The role of non-equilibrium vibrational structures in electronic coherence and recoherence in pigment-protein complexes, *Nat. Phys.* **9**, 113 (2013).
- [14] J. Iiles-Smith, A. G. Dijkstra, N. Lambert, and A. Nazir, Energy transfer in structured and unstructured environments: Master equations beyond the Born-Markov approximations, *J. Chem. Phys.* **144**, 044110 (2016).
- [15] J. del Pino, F. A. Y. N. Schröder, A. W. Chin, J. Feist, and F. J. Garcia-Vidal, Tensor Network Simulation of Non-Markovian Dynamics in Organic Polaritons, *Phys. Rev. Lett.* **121**, 227401 (2018).

- [16] J. del Pino, F. A. Y. N. Schröder, A. W. Chin, J. Feist, and F. J. Garcia-Vidal, Tensor network simulation of polaron-polaritons in organic microcavities, *Phys. Rev. B* **98**, 165416 (2018).
- [17] C. Clear, R. C. Schofield, K. D. Major, J. Iles-Smith, A. S. Clark, and D. P. S. McCutcheon, Phonon-Induced Optical Dephasing in Single Organic Molecules, *Phys. Rev. Lett.* **124**, 153602 (2020).
- [18] J. A. Ćwik, S. Reja, P. B. Littlewood, and J. Keeling, Polariton condensation with saturable molecules dressed by vibrational modes, *Europhys. Lett.* **105**, 47009 (2014).
- [19] F. C. Spano, Optical microcavities enhance the exciton coherence length and eliminate vibronic coupling in j-aggregates, *J. Chem. Phys.* **142**, 184707 (2015).
- [20] J. Galego, F. J. Garcia-Vidal, and J. Feist, Cavity-Induced Modifications of Molecular Structure in the Strong-Coupling Regime, *Phys. Rev. X* **5**, 041022 (2015).
- [21] F. Herrera and F. C. Spano, Cavity-Controlled Chemistry in Molecular Ensembles, *Phys. Rev. Lett.* **116**, 238301 (2016).
- [22] N. Wu, J. Feist, and F. J. Garcia-Vidal, When polarons meet polaritons: Exciton-vibration interactions in organic molecules strongly coupled to confined light fields, *Phys. Rev. B* **94**, 195409 (2016).
- [23] F. Herrera and F. C. Spano, Absorption and photoluminescence in organic cavity QED, *Phys. Rev. A* **95**, 053867 (2017).
- [24] F. Herrera and F. C. Spano, Dark vibronic polaritons and the spectroscopy of organic microcavities, *Phys. Rev. Lett.* **118**, 223601 (2017).
- [25] M. A. Zeb, P. G. Kirton, and J. Keeling, Exact states and spectra of vibrationally dressed polaritons, *ACS Photonics* **5**, 249 (2018).
- [26] A. Strashko, P. Kirton, and J. Keeling, Organic Polariton Lasing and the Weak to Strong Coupling Crossover, *Phys. Rev. Lett.* **121**, 193601 (2018).
- [27] K. B. Arnardottir, A. J. Moilanen, A. Strashko, P. Törmä, and J. Keeling, Multimode Organic Polariton Lasing, *Phys. Rev. Lett.* **125**, 233603 (2020).
- [28] A. Strathearn, P. Kirton, D. Kilda, J. Keeling, and B. W. Lovett, Efficient Non-Markovian Quantum Dynamics using Time-Evolving Matrix Product Operators, *Nat. Commun.* **9**, 3322 (2018).
- [29] F. A. Pollock, C. Rodríguez-Rosario, T. Frauenheim, M. Paternostro, and K. Modi, Non-Markovian quantum processes: Complete framework and efficient characterization, *Phys. Rev. A* **97**, 012127 (2018).
- [30] M. R. Jørgensen and F. A. Pollock, Exploiting the Causal Tensor Network Structure of Quantum Processes to Efficiently Simulate Non-Markovian Path Integrals, *Phys. Rev. Lett.* **123**, 240602 (2019).
- [31] G. E. Fux, E. P. Butler, P. R. Eastham, B. W. Lovett, and J. Keeling, Efficient Exploration of Hamiltonian Parameter Space for Optimal Control of Non-Markovian Open Quantum Systems, *Phys. Rev. Lett.* **126**, 200401 (2021).
- [32] M. Cygorek, M. Cosacchi, A. Vagov, V. M. Axt, B. W. Lovett, J. Keeling, and E. M. Gauger, Simulation of open quantum systems by automated compression of arbitrary environments, *Nat. Phys.* **18**, 662 (2022).
- [33] A. Bose and P. L. Walters, A multisite decomposition of the tensor network path integrals, *J. Chem. Phys.* **156**, 024101 (2022).
- [34] M. Richter and S. Hughes, Enhanced TEMPO Algorithm for Quantum Path Integrals with Off-Diagonal System-Bath Coupling: Applications to Photonic Quantum Networks, *Phys. Rev. Lett.* **128**, 167403 (2022).
- [35] H.-P. Breuer and F. Petruccione, *The Theory of Open Quantum Systems* (Oxford University Press, New York, 2002).
- [36] See Supplemental Material at <http://link.aps.org/supplemental/10.1103/PhysRevLett.129.173001> for discussion of: The weak system-environment coupling limit, the derivation of the mean-field equations, bright and dark states in mean-field theory, the implementation with PT-TEMPO and broader applicability of the approach, fitting procedures used for Figs. 2 and 3, the weak light-matter coupling theory of the model, comparison to an effective Holstein-Tavis-Cummings model, the multimode model and momentum-dependent spectra, and inverse Green's functions in the normal state, which includes Refs. [37–60].
- [37] H. Haken, The semiclassical and quantum theory of the laser, in *Quantum Optics Proceedings of the Tenth Session of the Scottish Universities Summer School in Physics, 1969*, edited by S. M. Kay and A. Maitland (Academic Press Inc., London, 1970), pp. 201–322.
- [38] J. del Pino, J. Feist, and F. J. Garcia-Vidal, Quantum theory of collective strong coupling of molecular vibrations with a microcavity mode, *New J. Phys.* **17**, 053040 (2015).
- [39] L. A. Martínez-Martínez and J. Yuen-Zhou, Comment on ‘Quantum theory of collective strong coupling of molecular vibrations with a microcavity mode’, *New J. Phys.* **20**, 018002 (2018).
- [40] J. del Pino, J. Feist, and F. J. Garcia-Vidal, Reply to the Comment on ‘Quantum theory of collective strong coupling of molecular vibrations with a microcavity mode’, *New J. Phys.* **20**, 018001 (2018).
- [41] P. M. Chaikin and T. C. Lubensky, *Principles of Condensed Matter Physics*, 1st ed. (Cambridge University Press, Cambridge, England, 1995).
- [42] A. Wipf, *Statistical Approach to Quantum Field Theory: An Introduction*, 2nd ed. (Springer International Publishing, Cham, 2021).
- [43] S. Krämer and H. Ritsch, Generalized mean-field approach to simulate the dynamics of large open spin ensembles with long range interactions, *Eur. Phys. J. D* **69**, 282 (2015).
- [44] R. F. Ribeiro, L. A. Martínez-Martínez, M. Du, J. Campos-Gonzalez-Angulo, and J. Yuen-Zhou, Polariton chemistry: Controlling molecular dynamics with optical cavities, *Chem. Sci.* **9**, 6325 (2018).
- [45] Extensions of this concept can also be made for models including a continuum of in-plane cavity modes; a similar division survives as long as the number of low energy photon modes is much smaller than the number of molecules [1,76–78].
- [46] R. P. Feynman and F. L. Vernon, The theory of a general quantum system interacting with a linear dissipative system, *Ann. Phys. (N.Y.)* **24**, 118 (1963).
- [47] N. Makri and D. E. Makarov, Tensor propagator for iterative quantum time evolution of reduced density matrices. I. Theory, *J. Chem. Phys.* **102**, 4600 (1995).

- [48] N. Makri and D. E. Makarov, Tensor propagator for iterative quantum time evolution of reduced density matrices. II. Numerical methodology, *J. Chem. Phys.* **102**, 4611 (1995).
- [49] R. Orús, A practical introduction to tensor networks: Matrix product states and projected entangled pair states, *Ann. Phys. (Amsterdam)* **349**, 117 (2014).
- [50] D. Gribben, A. Strathearn, G. E. Fux, P. Kirton, and B. W. Lovett, Using the environment to understand non-Markovian open quantum systems, [arXiv:2106.04212](https://arxiv.org/abs/2106.04212).
- [51] T. E. Lee, S. Gopalakrishnan, and M. D. Lukin, Unconventional Magnetism via Optical Pumping of Interacting Spin Systems, *Phys. Rev. Lett.* **110**, 257204 (2013).
- [52] J. Jin, A. Biella, O. Viyuela, L. Mazza, J. Keeling, R. Fazio, and D. Rossini, Cluster Mean-Field approach to the Steady-State Phase Diagram of Dissipative Spin Systems, *Phys. Rev. X* **6**, 031011 (2016).
- [53] R. Rota, F. Storme, N. Bartolo, R. Fazio, and C. Ciuti, Critical behavior of dissipative two-dimensional spin lattices, *Phys. Rev. B* **95**, 134431 (2017).
- [54] D. Huybrechts, F. Minganti, F. Nori, M. Wouters, and N. Shammah, Validity of mean-field theory in a dissipative critical system: Liouvillian gap, \mathbb{PT} -symmetric antgap, and permutational symmetry in the XYZ model, *Phys. Rev. B* **101**, 214302 (2020).
- [55] S. Gopalakrishnan, B. L. Lev, and P. M. Goldbart, Emergent crystallinity and frustration with Bose–Einstein condensates in multimode cavities, *Nat. Phys.* **5**, 845 (2009).
- [56] S. Gopalakrishnan, B. L. Lev, and P. M. Goldbart, Atom-light crystallization of Bose–Einstein condensates in multimode cavities: Nonequilibrium classical and quantum phase transitions, emergent lattices, supersolidity, and frustration, *Phys. Rev. A* **82**, 043612 (2010).
- [57] M. Kasha, Characterization of electronic transitions in complex molecules, *Discuss. Faraday Soc.* **9**, 14 (1950).
- [58] D. Meiser, J. Ye, D. R. Carlson, and M. J. Holland, Prospects for a Millihertz-Linewidth laser, *Phys. Rev. Lett.* **102**, 163601 (2009).
- [59] E. Eizner, L. A. Martínez-Martínez, J. Yuen-Zhou, and S. Kéna-Cohen, Inverting singlet and triplet excited states using strong light-matter coupling, *Sci. Adv.* **5**, eaax4482 (2019).
- [60] M. H. Szymańska, J. Keeling, and P. B. Littlewood, Mean-field theory and fluctuation spectrum of a pumped decaying Bose–Fermi system across the quantum condensation transition, *Phys. Rev. B* **75**, 195331 (2007).
- [61] T. Mori, Exactness of the mean-field dynamics in optical cavity systems, *J. Stat. Mech.* (2013) P06005.
- [62] F. Carollo and I. Lesanovsky, Exactness of Mean-Field Equations for Open Dicke Models with an Application to Pattern Retrieval Dynamics, *Phys. Rev. Lett.* **126**, 230601 (2021).
- [63] R. Houdré, R. P. Stanley, and M. Illegems, Vacuum-field Rabi splitting in the presence of inhomogeneous broadening: Resolution of a homogeneous linewidth in an inhomogeneously broadened system, *Phys. Rev. A* **53**, 2711 (1996).
- [64] P. R. Eastham and P. B. Littlewood, Bose condensation of cavity polaritons beyond the linear regime: The thermal equilibrium of a model microcavity, *Phys. Rev. B* **64**, 235101 (2001).
- [65] J. A. Ćwik, P. Kirton, S. De Liberato, and J. Keeling, Excitonic spectral features in strongly coupled organic polaritons, *Phys. Rev. A* **93**, 033840 (2016).
- [66] A. Strathearn, *Modelling Non-Markovian Quantum Systems Using Tensor Networks*, Springer Theses (Springer International Publishing, Cham, 2020).
- [67] The TEMPO Collaboration, OQuPy: A Python 3 package to efficiently compute non-Markovianopen quantum systems (2020), [10.5281/zenodo.4428316](https://doi.org/10.5281/zenodo.4428316).
- [68] P. Kirton, M. M. Roses, J. Keeling, and E. G. Dalla Torre, Introduction to the Dicke Model: From Equilibrium to Nonequilibrium, and Vice Versa, *Adv. Quantum Technol.* **2**, 1800043 (2019).
- [69] F. P. Schäfer, *Dye Lasers* (Springer-Verlag, New York, 1990).
- [70] P. Kirton and J. Keeling, Superradiant and lasing states in driven-dissipative dicke models, *New J. Phys.* **20**, 015009 (2018).
- [71] P. Kirton and J. Keeling, Thermalization and breakdown of thermalization in photon condensates, *Phys. Rev. A* **91**, 033826 (2015).
- [72] J. Keeling, M. H. Szymańska, and P. B. Littlewood, Keldysh Green’s function approach to coherence in a non-equilibrium steady state: Connecting Bose–Einstein condensation and lasing, in *Optical Generation and Control of Quantum Coherence in Semiconductor Nanostructures*, NanoScience and Technology, edited by G. Slavcheva and P. Roussignol (Springer, Berlin, Heidelberg, 2010).
- [73] We denote this as spectral weight rather than absorption, as the absorption spectral of a general lossy cavity is a more complicated expression, see Refs. [65,74] for discussion.
- [74] C. Ciuti and I. Carusotto, Input-output theory of cavities in the ultrastrong coupling regime: The case of time-independent cavity parameters, *Phys. Rev. A* **74**, 033811 (2006).
- [75] J. Keeling, P. R. Eastham, M. H. Szymanska, and P. B. Littlewood, Polariton Condensation with Localized Excitons and Propagating Photons, *Phys. Rev. Lett.* **93**, 226403 (2004).
- [76] V. M. Agranovich, M. Litinskaya, and D. G. Lidzey, Cavity polaritons in microcavities containing disordered organic semiconductors, *Phys. Rev. B* **67**, 085311 (2003).
- [77] P. Michetti and G. C. La Rocca, Polariton states in disordered organic microcavities, *Phys. Rev. B* **71**, 115320 (2005).
- [78] L. A. Martínez-Martínez, E. Eizner, S. Kéna-Cohen, and J. Yuen-Zhou, Triplet harvesting in the polaritonic regime: A variational polaron approach, *J. Chem. Phys.* **151**, 054106 (2019).
- [79] P. Fowler-Wright, J. M. J. Keeling, and B. W. Lovett, Data underpinning: Efficient many-body non-Markovian dynamics of organic polaritons, [10.17630/27aa0850-9bd6-442b-abf7-49434c061464](https://doi.org/10.17630/27aa0850-9bd6-442b-abf7-49434c061464) (2022).